Korean J. Chem. Eng., 34(5), 1517-1523 (2017)
DOI: 10.1007/s11814-017-0013-5

pISSN: 0256-1115
eISSN: 1975-7220

Effects of solvents on rheological and crosslinking properties of photo-polymerized poly(ethylene glycol) hydrogels

Kevin Injoe Jung*, Dong Geun Lee*, Ki Wan Bong*, Seung Man Noh, Min Seop Um***, Woo Jin Choi***, Bumsang Kim****,†, and Hyun Wook Jung*,†**

*Department of Chemical and Biological Engineering, Korea University, Seoul 02841, Korea
**Research Center for Green Fine Chemicals, Korea Research Institute of Chemical Technology, Ulsan 44412 Korea
***Chemical Materials Solutions Center, Korea Research Institute of Chemical Technology, Daejeon 34114, Korea
****Department of Chemical Engineering, Hongik University, Seoul 04066, Korea
(*Received 19 August 2016 • accepted 2 February 2017*)

Abstract−The effects of solvents such as water and ethanol on the rheological properties and crosslinking characteristics of poly(ethylene glycol) (PEG) hydrogels were examined. Real-time storage modulus data for pre-polymerized mixtures containing different solvents during the photo-polymerization process successfully explained the differences in the formation of crosslinked networks of the corresponding hydrogels. Various experimental methods for Fourier transform infrared spectroscopy (FT-IR), swelling ratio, Rhodamine-B (Rh-B) loading/release properties, and scratch/indentation depths on hydrogel surfaces, were employed to systematically compare macroscopic structural and mechanical properties of the crosslinked PEG hydrogels with different solvents (water and ethanol). The effects of the solvents on the hydrogel properties were satisfactorily consistent, and the results clearly indicated that water hindered the formation of the crosslinked network more severely than ethanol at the same weight ratio because of the presence of larger number of water molecules in pre-polymerized mixtures, which was a more favorable feature for water than ethanol in the initial crosslinking growth.

Keywords: PEG Hydrogels, Rheology, Photo-polymerization, Solvent Effect, Crosslinking, Elastic Modulus, Scratch and Indentation Depths

INTRODUCTION

Hydrogels have received considerable attention for chemical, biomedical, and pharmaceutical applications because of their hydrophilic nature and biocompatibility [1-6]. Polymer hydrogels have three-dimensional crosslinked networks that can absorb large amounts of water or aqueous solvents, yet are insoluble owing to the presence of dense crosslinks. These crosslinked networks are mainly formed by free-radical polymerization, known as gelation or crosslinking. The network properties, such as the mesh size and rheological/mechanical properties, are key factors affecting the specific bio-related applications of polymerized hydrogels. For example, the mesh size of crosslinked hydrogels in drug delivery systems or electrophoresis gels and the mechanical properties of hydrogels as antifouling coating materials on the membranes or bone regeneration scaffolds play important roles [7-9]; thus, it is desirable to tune the hydrogel characteristics. However, the study of the crosslinked network properties of hydrogels has been still regarded as unimportant.

Among the various techniques for investigating the network properties of polymeric hydrogels, real-time rheological measurements, such as elastic and viscous moduli (G′ and G″), during the gelation process from liquid- to solid-like phases, can offer beneficial information about the evolution of crosslinked hydrogels. Few reports have rheologically interpreted the relationship between the real-time crosslinking kinetics and mechanical/structural features of completely crosslinked hydrogel samples [10-16]. Employing rheological measurement method, in particular, will be important for elucidating the role of solvents in the crosslinking process for the control of the crosslinking density and the porous structure of hydrogels applied in drug delivery and membranes [17-21].

Thus, our primary purpose was to scrutinize the effects of solvents in pre-polymerized mixtures on the network properties of polymeric hydrogels by monitoring the in-situ rheological evolution of poly(ethylene glycol) (PEG) hydrogels during UV photo-polymerization process to optimally tune hydrogels for customized applications. PEG is an attractive hydrogel that has been employed extensively for many applications, such as tissue engineering, drug delivery devices, bioseparation, and antifouling membranes. PEG is reputed for its biocompatibility, capability to make drugs soluble, role in hiding drug-circulating systems from immune recognition (especially in the liver), good protein- and cell-resistant properties, non-serious interaction with blood- and cellular proteins, and relatively easy excretion from the body [22-29]. Two kinds of solvents, water and ethanol, were included in PEG pre-polymer-

†To whom correspondence should be addressed.
E-mail: hwjung@grtrkr.korea.ac.kr, bskim@hongik.ac.kr
‡This paper is dedicated to Professor Sung Hyun Kim for commemorating his retirement from Department of Chemical and Biological Engineering of Korea University.

ized mixtures. Water is known for effectively reducing the activation energy in the polymerization process owing to its hydrogen-bonding nature. Ethanol, whose molecules are larger than those of water, affects the movement of radicals [30-32]. The effects of these two solvents dispersed at a low concentration in pre-polymerized mixtures on the crosslinking evolution for PEG hydrogels were investigated, using real-time rheological tests in the small amplitude oscillatory shear (SAOS) mode [33-35]. Fourier transform infrared (FT-IR) data were obtained at a wavelength 1,637 cm^{-1} for the temporal change of methacrylate double bonds, which were supported by the rheological results at different irradiation times [36]. The final properties of the crosslinked PEG hydrogels produced from rheological tests, such as the water swelling ratio and Rh-B uptake/release amounts, were macroscopically examined [37]. The mechanical properties of the crosslinked hydrogel films, e.g., scratch and indentation depths on the film surface, were estimated by nano-scratch [38,39] and ultra-nano-indentation tests [40].

EXPERIMENTAL

1. Preparation of Pre-polymerized Mixtures Including Solvents

Poly(ethylene glycol) methacrylate (PEGMA, molecular weight=360) and poly(ethylene glycol) dimethacrylate (PEGDMA, molecular weight=330) were used as a monomer and a crosslinker, respectively, in the pre-polymerized mixtures for fabricating PEG hydrogels. The photo-initiator for the photo-polymerization process was 2,2-dimethoxy-2-phenylacetophenone (DMPA). The PEGMA and DMPA were obtained from Sigma-Aldrich. PEGDMA was purchased from Tokyo Chemical Industry (Japan).

The molar ratio of the monomer to the crosslinker was set as 1 : 1. Water (W) or ethanol (Et) was included as a solvent by varying its weight fraction for each test, to determine the effects of these solvents on the real-time rheological and crosslinking properties of PEG hydrogels. A small amount of DMPA was finally added to the mixtures (1 wt% of above three compositions). The detailed formulations for the pre-polymerized mixtures are listed in Table 1. Note that two pre-polymerized samples containing solvents mixed with water and ethanol were additionally prepared to compare their rheological properties with those by samples with single solvent.

Table 1. Formulations of pre-polymerized mixtures having two kinds of solvents (based on total amount of 3.03 g)

Sample	PEGMA (g)	PEGDMA (g)	DMPA (g)	Solvent (g)
S_0	1.5652	1.4348	0.03	0
S_{W10}	1.4087	1.2913	0.03	0.3
S_{W20}	1.2522	1.1478	0.03	0.6
S_{Et10}	1.4087	1.2913	0.03	0.3
S_{Et20}	1.2522	1.1478	0.03	0.6
S_{M10}	1.4087	1.2913	0.03	0.15(W)+0.15(Et)
S_{M20}	1.2522	1.1478	0.03	0.3(W)+0.3(Et)

2. Measurement of Real-time Rheological Properties During UV Polymerization

In previous studies, the rheological measurements performed during photo-polymerization supported the gelation or crosslinking characteristics of curable materials [10-16]. Real-time rheological data, including the storage or elastic modulus (G') growth, were recorded during the UV exposure using a rotational rheometer (MCR-301, Anton Paar, Austria) equipped with an external UV light source in the SAOS mode. The storage modulus data are highly related to the structural information of crosslinked hydrogels. The temperature and UV light intensity conditions were set equally for each pre-polymerized mixture to compare the micro-

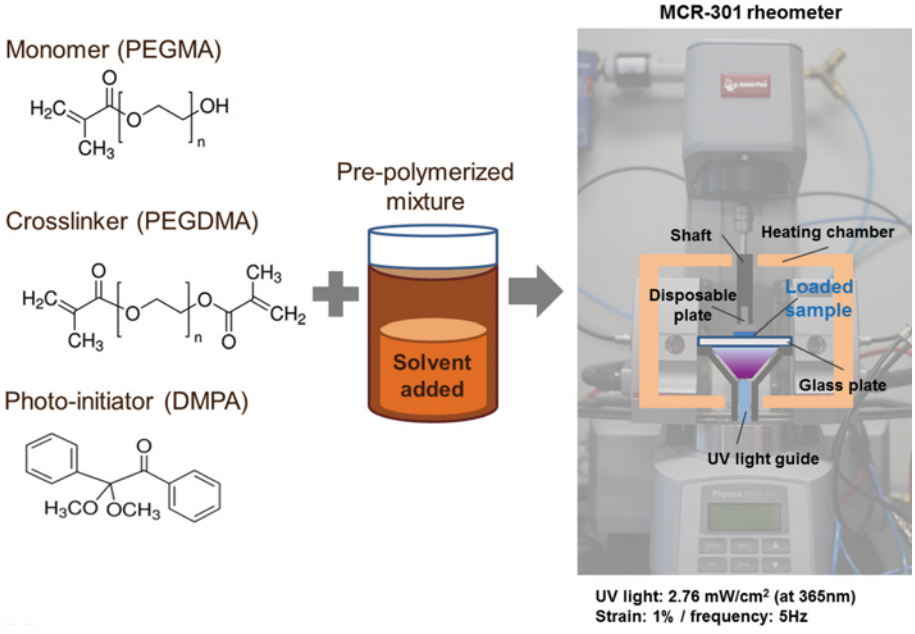

Fig. 1. Schematic diagram for rheological measurements of pre-polymerized mixtures with solvents (water or ethanol).

scopic-network formation during photo-polymerization. The temperature for the rheology test was maintained at 30 °C by the convection of heating/cooling air in a controlled temperature chamber. The UV light inducing the polymerization of the mixtures was emitted under the same intensity conditions: 0.42 mW/cm^2 at a wavelength of 313 nm and 2.76 mW/cm^2 at 365 nm.

Fig. 1 shows a schematic for measuring the rheological properties of the pre-polymerized samples listed in Table 1. The mixtures placed on the glass substrate were evenly exposed to UV light. The gap between the 8 mm upper-parallel plate and the glass plate was 300 μm (Note that same rheological data were obtained under 500 μm gap condition). The SAOS test was performed at a strain change of 1% within the linear viscoelastic regime and at an input frequency of 5 Hz because of the fast photo-polymerization.

3. Double-bond Conversion of PEG Hydrogels Indicated by Change in FT-IR Spectra

The crosslinking density of the polymer network was analyzed by examining the change in the C=C double bonds of PEGMA and PEGDMA using the transmittance mode of a Nicolet-6700 FT-IR spectrometer. The peak of the double bond appeared at 1,637 nm^{-1} in the IR band. The qualitative changes of the IR peaks were compared for samples with different portions of solvents and were extracted at varying rheological measurement times: 0 s (before the test), 75 s, and 300 s (after the test).

4. Swelling Ratio and Rh-B Incorporation/Release Analysis of PEG Hydrogels

The water-swelling characteristics of the disk-like PEG hydrogel films were examined after the photo-polymerization via rheology tests. The films were dried in a vacuum oven for 24 h at 80 °C. The dried samples were weighed and then soaked in distilled water at room temperature for 72 h. The swollen film was removed from the water and weighed again after the wetted surfaces were carefully wiped. The water-swelling ratio of a hydrogel film is defined as

$$q=W_s/W_d, \quad (1)$$

where W_s and W_d are the weights of the swollen hydrogel after swelling test and the initial dried hydrogel before the swelling test, respectively.

We prepared a 0.05 mM Rh-B (Rhodamine B) stock solution and measured its absorbance at a wavelength of 554 nm using a UV-visible spectrophotometer (Varian, Cary100). Rh-B was incorporated into the crosslinked hydrogels by soaking the crosslinked hydrogel disks in 20 mL of the Rh-B stock solution. After 24 h, 0.5 mL samples were removed from the solution, and their absorbance was measured to determine the loading amount of Rh-B. The Rh-B-loaded hydrogel disks were separated from the solution by centrifugation and then used for release experiments. To release the Rh-B from the hydrogels, Rh-B-loaded hydrogel disks were placed in PBS of 25 ml. After 24 h, a 0.5 mL sample was withdrawn from the solution, and its absorbance was measured. The amounts of incorporated and released Rh-B were determined using the calibration curve of the Rh-B concentrations versus the absorbance [37].

5. Mechanical Properties of Final Crosslinked PEG Hydrogels

The mechanical resistance at the surface of 300 μm-thick crosslinked hydrogels, produced from rheological tests, was measured using a nano-scratch tester (Anton Paar Tritec SA, Switzerland). A normal force ranging from 1 to 20 mN was progressively applied on the surface of the hydrogel film along a horizontal scratch 1 mm in length at a scratch speed of 2 mm/min. A sphero-conical nano scratch tip with an indenter radius of 2 μm and a cone angle of 90° was used for all the scratch tests [38,39]. A nano-indentation tester (Anton Paar Tritec SA, Switzerland) was used to estimate the mechanical hardness of the hydrogel film surface according to an indentation load-displacement curve [40]. A Berkovich diamond tip was used to perform indentation tests. A maximum indentation load of 2,000 μN was imposed, considering the relatively low vertical penetration depth needed to exclude the substrate effect. The rate of loading and unloading of the indentation tip was set as 4,000 μN/min.

RESULTS AND DISCUSSION

1. Real-time Rheological Characteristics of Pre-polymerized Samples During UV Irradiation Process

The gelation process for the PEG hydrogels was investigated in real-time rheological tests by measuring the storage modulus (G′) of pre-polymerized samples with different amounts of solvents. Storage modulus data obtained from a rheometer equipped with a UV module provided useful information about the crosslinking behaviors of hydrogels [10-16,33-35]. G′ could not be detected before the onset of crosslinking because there was no significant elastic contribution in the primitive samples.

In this study, the type and amount of solvents dispersed in the pre-polymerized solutions were the factors affecting the crosslinking characteristics, such as the onset time, transient response of G′, and final G′ values at the end of irradiation (300 s). The evolution of the elastic modulus for various samples, which directly represents the crosslinked network development, is illustrated in Fig. 2(a). The sample without any solvent, S_0, had the fastest crosslinking onset time and reached the highest final G′ value at the highest crosslinking rate. This is due to the absence of hindrance by a solvent at the crosslinking reaction stage. As the amount of solvent within the samples increased, the final G′ value gradually decreased (Fig. 2(b)). The final G′ data indicate that the ethanol solvent hindered the crosslinking formation less than the water solvent at the same weight concentration. Interestingly, however, the temporal crosslinking rate of water was larger than that of ethanol. This is because water triggered the crosslinking formation of hydrogels to a greater extent than ethanol due to its hydrogen-bonding feature [31,32], but the large number of water molecules compared with the number of ethanol molecules caused greater disturbance of the crosslinking at the same weight ratio. For the record, real-time rheological data for samples (S_{M10} and S_{M20}) including both water and ethanol solvents were compared with those by samples with single solvents. For instance, the initial crosslinking rate of S_{M10} was similar to that of S_{W10} due to the hydrogen bonds [41], whereas its final G′ was lower than those of both S_{W10} and S_{Et10}, exhibiting the negative effect of solvent mixing on the rheological property.

Note that a pre-polymerized mixture with 20 wt% of the water solvent, S_{W20}, was very turbid owing to the phase separation caused by the low solubility of water [6], as shown in Fig. 3(a) (in con-

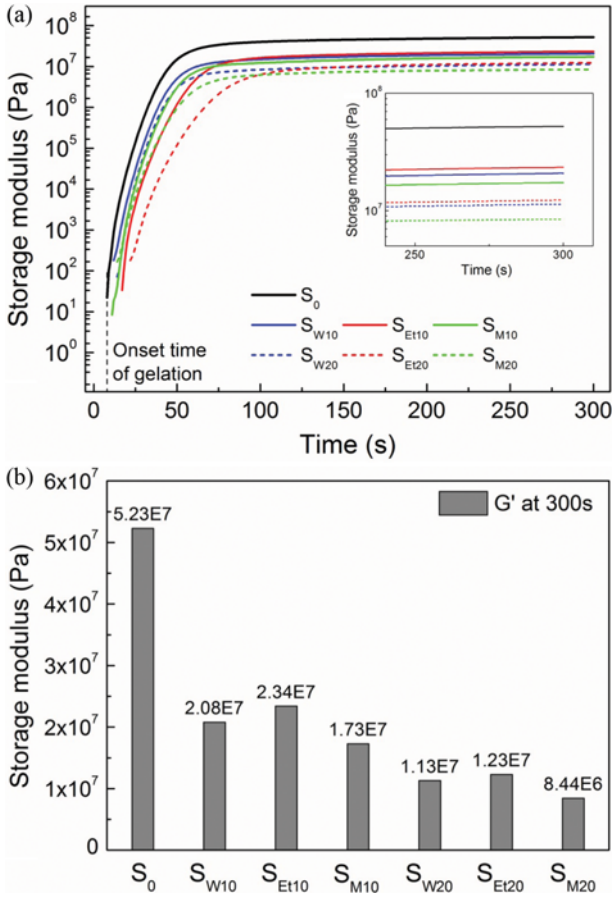

Fig. 2. (a) Evolution of storage modulus for pre-polymerized samples listed in Table 1 and (b) their final storage modulus values at UV irradiation end time.

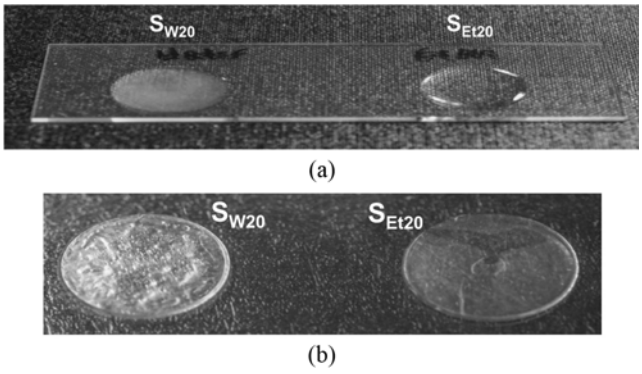

Fig. 3. Photographs of (a) pre-polymerized samples, S_{W20} and S_{Et20} before the rheology test and (b) their crosslinked samples after the rheology test.

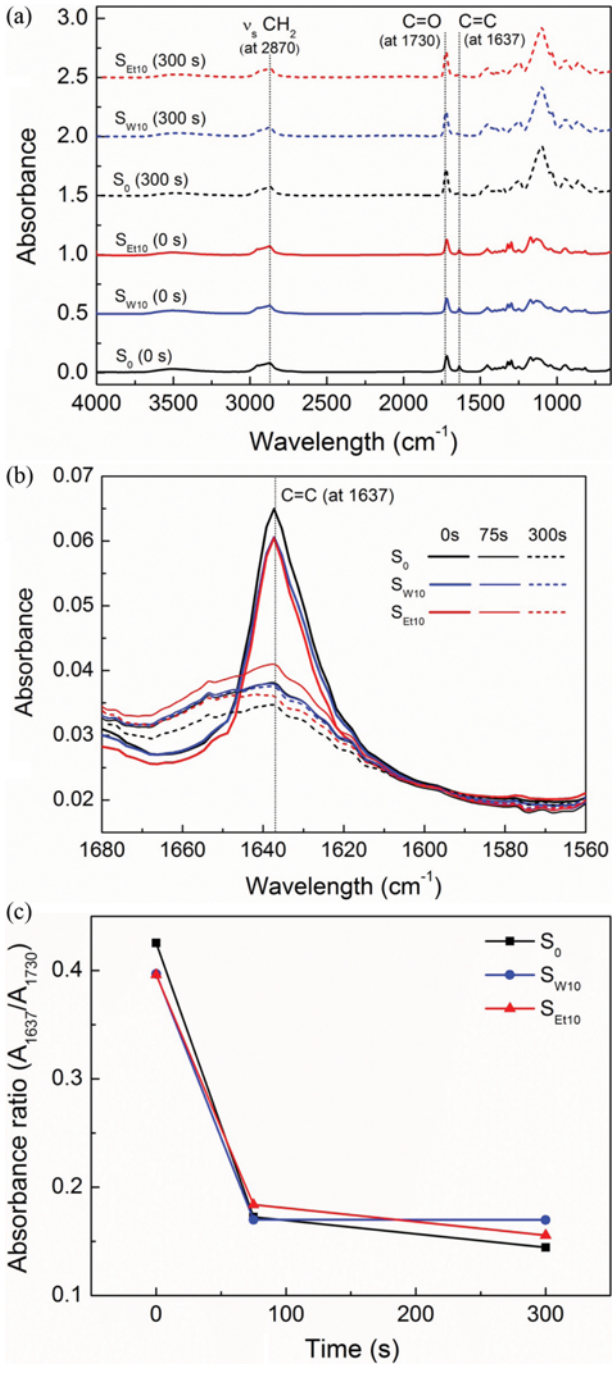

Fig. 4. IR peaks of samples for S_0, S_{W10}, and S_{Et10} (a) in the wide range of wavelength, (b) near wavelength 1,637 cm^{-1}. (c) Absorbance ratio between IR peaks at 1,637 cm^{-1} and 1,730 cm^{-1}.

trast, S_{Et20} was still transparent.), resulting in the uneven shape of the fully crosslinked sample for S_{W20} (Fig. 3(b)). For this reason, we mainly focused on samples with a solvent concentration of 10 wt% in describing the subsequent experimental results.

2. Variation of Double Bonds Inside PEG Hydrogels During UV Irradiation through FT-IR Analysis

IR peaks of samples exposed to UV light for different durations - 0, 75, and 300 s, were measured to qualitatively interpret the change of the double bond amount during the free-radical polymerization process. In Fig. 4(a), two overall IR absorption peaks for three mixtures without a solvent and with a solvent at a concentration of 10 wt% (S_0, S_{W10}, and S_{Et10}) are observed at a wavelength of 1,637 cm^{-1} for the vibration of C=C double bonds on methacrylate groups (symmetric methylene stretching, ν_s CH_2) at 2,870 cm^{-1} and carbonyl groups (C=O) at 1,730 cm^{-1} for unre-

acted groups. The heights of the peaks at 1,637 cm^{-1} (Fig. 4(b)) and the absorbance ratios between peaks at 1,637 cm^{-1} and 1,730 cm^{-1} for various samples (Fig. 4(c)) indicate the relative quantities of remnant double bonds at the pre-irradiation (0 s), intermediate (75 s), and post-irradiation (300 s) stages. The G′ data in Fig. 2(a) are nearly constant around the UV irradiation time of 75 s. In the non-UV irradiation stage, the peak height for sample S_0 without a solvent was naturally more than that for samples containing solvents because of the larger amounts of PEGMA and PEGDMA in S_0. The mixtures with the same amounts of solvents exhibited similar peaks, which were lower than that of S_0.

At the given UV exposure times (75 and 300 s), the IR absorbance differed among the samples, clarifying the effects of the solvents on the photo-polymerization process. The crosslinked PEG hydrogel without a solvent (at 300 s) exhibited the highest reduction of double bonds owing to the formation of a denser crosslinking network. In comparison, the solvent-containing hydrogels had a less-dense structure, possibly because of the interruption of the crosslinking by the solvents during the polymerization process.

After 300 s of UV irradiation, the peak for S_{W10} was higher than that for S_{Et10}, indicating that the water solvent hindered the gelation process slightly more than the ethanol solvent. However, at the intermediate irradiation time of 75 s, two samples showed the opposite trend: the peak for S_{Et10} was higher than that for S_{W10}. This clearly demonstrates the low crosslinking rate of the S_{Et10} sample, as addressed in Fig. 2.

3. Swelling Ratio and Rh-B Incorporation/Release Features of Hydrogels Networks

PEG hydrogel films produced from rheology tests were used for macroscopic structure analysis. The change in the crosslinking density inside the hydrogel films with respect to the type and amount of solvent was estimated according to the water-swelling ratio and Rh-B loading/release properties. Fig. 5(a) shows that the PEG hydrogels absorbed more water when the amount of solvent increased, indicating that a relatively low-dense crosslinking network was formed by the solvent. The inclusion of a solvent in a pre-polymerized mixture can cause a less-dense crosslinked network by providing space between the crosslinks during the polymerization process. A comparison of the swelling ratio at the same solvent weight ratio proves that the water solvent hindered the crosslinking formation more than the ethanol solvent, which is consistent with previous rheology and FT-IR tests.

The uptake and release amounts of Rh-B in various PEG hydrogels made from the rheology test showed similar patterns, as was the case for the swelling ratio test (Fig. 5(b)). The loading/release amounts of Rh-B were very low in the hydrogel of S_0, which had no solvent, because of the formation of a dense crosslinked network. They were slightly higher for S_{W10} than for S_{Et10} at the same solvent concentration, which agrees with previous results.

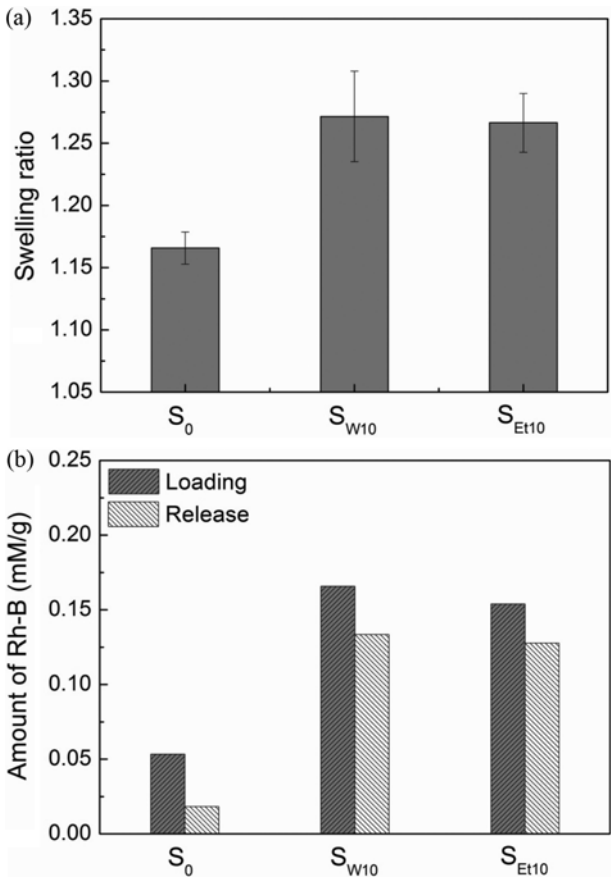

Fig. 5. (a) Water swelling ratios and (b) Rh-B incorporation/release properties for crosslinked samples, S_0, S_{W10}, and S_{Et10}.

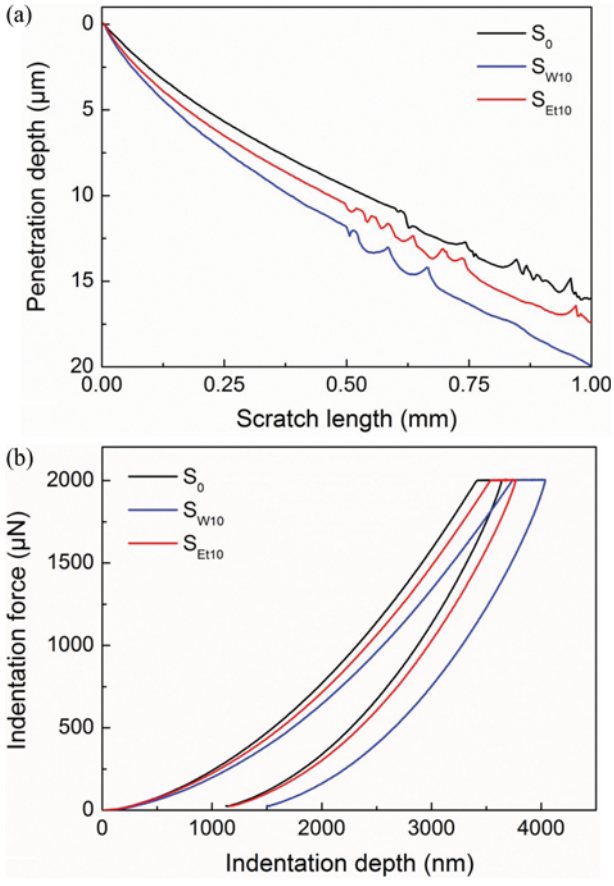

Fig. 6. (a) Scratch penetration depths from nano scratch test and (b) indentation depths from ultra-nano indentation test for crosslinked samples, S_0, S_{W10}, and S_{Et10}.

4. Mechanical Strength of PEG Hydrogel Films

The scratch and indentation depth properties of crosslinked PEG hydrogel films were compared via nano scratch and ultra-nano indentation tests of the film surfaces. Fig. 6(a) depicts the penetration depth profiles on the film surfaces of the crosslinked samples - S_0, S_{W10}, and S_{Et10} - along a horizontal movement up to 1mm of the vertical-load tip under the progressive loading from 0.5 to 20 mN. The mechanical strength is directly correlated to the penetration depth on the surface of the hydrogel film. In general, a soft film with a less-dense crosslinked structure suffers deeper scratches or mars than a hard one. The scratch resistance properties of hydrogels with different types and amounts of solvents exhibited a similar trend to the final storage modulus data for the hydrogels: smaller and larger penetration depths for the S_0 (without any solvent) and S_{W10} hydrogels, respectively.

The hardness of crosslinked hydrogel films was measured in an ultra-nano indentation test. Under the vertical load range of 0 to 2,000 μN, there were clear differences among the indentation depth profiles of the S_0, S_{W10}, and S_{Et10} hydrogels (Fig. 6(b)), which agree with the scratch results. According to the level of the crosslinked network structure of the hydrogels, the indentation depth for the S_0 hydrogel was smaller than that of S_{W10} and S_{Et10} under the same loading condition. The S_{Et10} hydrogel, which had a denser crosslinked structure than S_{W10}, gave a smaller indentation depth.

Real-time rheological data regarding the development of the crosslinked network inside PEG hydrogels during the gelation process are highly useful for elucidating the final mechanical and macroscopic structural properties of crosslinked hydrogel systems with controlled solvents.

CONCLUSION

The fundamental properties of hydrogels can be desirably tuned for many applications by controlling the space between crosslinks during the gelation process via a solvent. The effects of water and ethanol solvents on the rheological and crosslinking properties of PEG hydrogels were examined. The addition of water or ethanol to pre-polymerized mixtures produced less-dense crosslinked networks in hydrogels compared to the case without a solvent. At the same weight ratio, the water solvent disturbed the final crosslinking of hydrogels more than the ethanol solvent, although it increased the free-radical polymerization rate at the early stage of crosslinking more than the ethanol solvent. This result was demonstrated by the real-time rheological properties (e.g., storage modulus) of pre-polymerized mixtures with different solvents during the photo-polymerization process. Real-time rheological data regarding the PEG hydrogels corroborated the different macroscopic structural and mechanical properties of the final crosslinked hydrogels with solvents, including the double bond change revealed by FT-IR, water swelling ratio, Rh-B loading/release properties, and scratch/indentation depths on hydrogel film surfaces.

ACKNOWLEDGEMENTS

This study was supported by the Ministry of Trade, Industry & Energy (MOTIE, Korea) under Industrial Technology Innovation Program (No. 10067082), the National Research Foundation of Korea (NRF) (NRF-2016R1A5A1009592 & NRF-2015R1D1A1A01056799), and Hongik University Research Fund.

REFERENCES

1. R. Langer and N. A. Peppas, *AIChE J.*, **49**, 2990 (2003).
2. N. Peppas, P. Bures, W. Leobandung and H. Ichikawa, *Eur. J. Pharm. Biopharm.*, **50**, 27 (2000).
3. E. Lee and B. Kim, *Korean J. Chem. Eng.*, **28**, 1347 (2011).
4. K. Chaturvedi, K. Ganguly, M. N. Nadagouda and T. M. Aminabhavi, *J. Control Release*, **165**, 129 (2013).
5. S. C. Lee, I. K. Kwon and K. Park, *Adv. Drug Delivery Rev.*, **65**, 17 (2013).
6. Y. H. Na, H. Y. Oh, Y. J. Ahn and Y. Han, *Korea-Aust. Rheol. J.*, **27**, 25 (2015).
7. J. A. Killion, L. M. Geever, D. M. Devine, J. E. Kennedy and C. L. Higginbotham, *J. Mech. Behav. Biomed.*, **4**, 1219 (2011).
8. H. Ju, B. D. McCloskey, A. C. Sagle, Y. H. Wu, V. A. Kusuma and B. D. Freeman, *J. Membr. Sci.*, **307**, 260 (2008).
9. R. A. Bader and W. E. Rochefort, *J. Biomed. Mater. Res. A.*, **86**, 494 (2008).
10. S. J. Buwalda, L. Calucci, C. Forte, P. J. Dijkstra and J. Feijen, *Polymer*, **53**, 2809 (2012).
11. R. Censi, P. J. Fieten, P. di Martino, W. E. Hennink and T. Vermonden, *Macromolecules*, **43**, 5771 (2010).
12. J. Wang and V. M. Ugaz, *Electrophoresis*, **27**, 3349 (2006).
13. C. A. Bonino, J. E. Samorezov, O. Jeon, E. Alsberg and S. A. Khan, *Soft Matter*, **7**, 11510 (2011).
14. S. Khan, I. Plitz and R. Frantz, *Rheol. Acta*, **31**, 151 (1992).
15. B. S. Chiou and S. A. Khan, *Macromolecules*, **30**, 7322 (1997).
16. J. W. Hwang, S. M. Noh, B. Kim and H. W. Jung, *J. Appl. Polym. Sci.*, **132**, 22 (2015).
17. G. Kang, Y. Cao, H. Zhao and Q. Yuan, *J. Membr. Sci.*, **318**, 227 (2008).
18. H. Ju, B. D. McCloskey, A. C. Sagle, V. A. Kusuma and B. D. Freeman, *J. Membr. Sci.*, **330**, 180 (2009).
19. H. Lin, T. Kai, B. D. Freeman, S. Kalakkunnath and D. S. Kalika, *Macromolecules*, **38**, 8381 (2005).
20. H. Lin, E. Van Wagner, J. S. Swinnea, B. D. Freeman, S. J. Pas, A. J. Hill, S. Kalakkunnath and D. S. Kalika, *J. Membr. Sci.*, **276**, 145 (2006).
21. H. Ju, B. D. McCloskey, A. C. Sagle, Y. H. Wu, V. A. Kusuma and B. D. Freeman, *J. Membr. Sci.*, **307**, 260 (2008).
22. S. J. Bryant and K. S. Anseth, *J. Biomed. Mater. Res.*, **59**, 63 (2002).
23. R. R. Hood, C. Shao, D. M. Omiatek, W. N. Vreeland and D. L. DeVoe, *Pharm. Res.*, **30**, 1597 (2013).
24. L. J. Suggs, M. S. Shive, C. A. Garcia, J. M. Anderson and A. G. Mikos, *J. Biomed Mater. Res.*, **46**, 22 (1999).
25. A. Dal Pozzo, L. Vanini, M. Fagnoni, M. Guerrini, A. De Benedittis and R. Muzzarelli, *Carbohyd. Polym.*, **42**, 201 (2000).
26. P. Roach, D. J. McGarvey, M. R. Lees and C. Hoskins, *Int. J. Mol. Sci.*, **14**, 8585 (2013).
27. G. Lin and B. Tarasevich, *J. Appl. Polym. Sci.*, **128**, 3534 (2013).
28. G. Tan, J. Liao, C. Ning and L. Zhang, *J. Appl. Polym. Sci.*, **125**, 3509 (2012).

29. Y. Ikeda, J. Katamachi, H. Kawasaki and Y. Nagasaki, *Bioconjugate Chem.*, **24**, 1824 (2013).
30. N. Ravi, A. Mitra, P. Hamilton and F. Horkay, *J. Polym. Sci. B: Polym. Phys.*, **40**, 2677 (2002).
31. A. Valdebenito and M. V. Encinas, *Polym. Int.*, **59**, 1246 (2010).
32. S. Beuermann, *Macromol. Rapid Commun.*, **30**, 1066 (2009).
33. M. B. Mellott, K. Searcy and M. V. Pishko, *Biomaterials*, **22**, 929 (2001).
34. A. M. Kloxin, A. M. Kasko, C. N. Salinas and K. S. Anseth, *Science*, **324**, 59 (2009).
35. F. M. Andreopoulos, E. J. Beckman and A. J. Russell, *Biomaterials*, **19**, 1343 (1998).
36. H. S. Mansur, R. L. Oréfice and A. A. Mansur, *Polymer*, **45**, 7193 (2004).
37. R. Zhang, M. Hummelgård, G. Lv and H. Olin, *Carbon*, **49**, 1126 (2011).
38. R. Consiglio, N. Randall, B. Bellaton and J. von Stebut, *Thin Solid Films*, **332**, 151 (1998).
39. S. M. Noh, J. W. Lee, J. H. Nam, K. H. Byun, J. M. Park and H. W. Jung, *Prog. Org. Coat.*, **74**, 257 (2012).
40. J. W. Hwang, K. N. Kim, S. M. Noh and H. W. Jung, *J. Coat. Technol. Res.*, **12**, 177 (2015).
41. K. Mizuno, Y. Miyashita and Y. Shindo, *J. Phys. Chem.*, **99**, 3225 (1995).